Event-by-event simulation of single-neutron experiments to test uncertainty relations

2014 Phys. Scr. 2014 014016

(http://iopscience.iop.org/1402-4896/2014/T163/014016)

IOP Publishing | Royal Swedish Academy of Sciences Physica Scripta

Phys. Scr. **T163** (2014) 014016 (7pp) doi:10.1088/0031-8949/2014/T163/014016

Event-by-event simulation of single-neutron experiments to test uncertainty relations*

H De Raedt[1] **and K Michielsen**[2,3]

[1] Department of Applied Physics, Zernike Institute for Advanced Materials, University of Groningen, Nijenborgh 4, NL-9747 AG Groningen, The Netherlands
[2] Institute for Advanced Simulation, Jülich Supercomputing Centre, Forschungszentrum Jülich, D-52425 Jülich, Germany
[3] RWTH Aachen University, D-52056 Aachen, Germany

E-mail: h.a.de.raedt@rug.nl and k.michielsen@fz-juelich.de

Received 19 December 2013, revised 10 March 2014
Accepted for publication 12 March 2014
Published 19 December 2014

Abstract

Results from a discrete-event simulation of a recent single-neutron experiment that tests Ozawa's generalization of Heisenberg's uncertainty relation are presented. The event-based simulation algorithm reproduces the results of the quantum theoretical description of the experiment but does not require the knowledge of the solution of a wave equation, nor does it rely on detailed concepts of quantum theory. In particular, the data from these non-quantum simulations satisfy uncertainty relations derived in the context of quantum theory.

Keywords: logical inference, quantum theory, inductive logic, probability theory

(Some figures may appear in colour only in the online journal)

Introduction

Quantum theory has proven extraordinarily powerful for describing a vast number of laboratory experiments, but it offers no rational, logically consistent explanation of how individual outcomes are produced. Of course, it is the human brain rather than a mathematical formalism which decides, on the basis of what it perceives through our senses and cognitive capabilities, what constitutes a definite answer. According to Bohr [1], 'Physics is to be regarded not so much as the study of something *a priori* given, but rather as the development of methods of ordering and surveying human experience. In this respect our task must be to account for such experience in a manner independent of individual subjective judgment and therefore objective in the sense that it can be unambiguously communicated in ordinary human language'. This quote suggests to constructing a description in terms of events, some of which are directly related to human experience, and the cause-and-effect relations among them. If such an event-based description reproduces the statistical results of experiments, it also provides a description on a level to which quantum theory has no access.

For many interference and entanglement phenomena observed in optics and neutron experiments, such an event-based description has already been constructed; see [2–4] for recent reviews. The event-based simulation models reproduce the statistical distributions of quantum theory without solving a wave equation, but by modeling physical phenomena as a chronological sequence of events. Here, events can be actions of an experimenter, particle emissions by a source, signal generations by a detector, interactions of a particle with a material and so on [2–4].

The basic premise of our event-based simulation approach is that current scientific knowledge derives from the discrete events which are observed in laboratory experiments and from relations between those events. Hence, the event-based simulation approach is concerned with how we can model these experimental observations, but not with what 'really' happens in Nature.

The general idea of the event-based simulation method is that simple rules define discrete-event processes which may lead to the behavior that is observed in experiments. The basic strategy in designing these rules is to carefully examine the experimental procedure and to devise rules such that they produce the same kind of data as those recorded in experiment, while avoiding the trap of simulating thought

* Invited paper presented at QTAP-6.

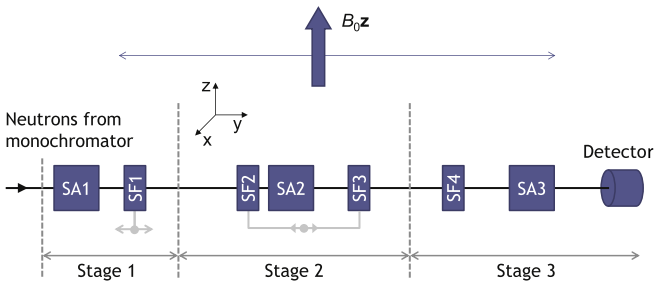

Figure 1. Functional block diagram of the neutron experiment [22, 23] for testing uncertainty relations; see also figure 2 in [22, 23]. Monochromatic neutrons enter from the left. SA1, SA2, SA3: spin analyzers (see the text); SF1, SF2, SF3, SF4: spin flippers (see the text). The positions of SF1 and the pair (SF2, SF3) are variable.

experiments that are difficult to realize in the laboratory. Evidently, mainly because of the lack of knowledge, the rules are not unique. Hence, it makes sense to use the simplest rules until a new experiment indicates that the rules should be modified. The method may be considered as entirely 'classical', since it only uses concepts which are directly related to our perception of the macroscopic world, but the rules themselves are not necessarily those of classical Newtonian dynamics.

The event-based approach has been successfully used for discrete-event simulations of the experiments with a single beam splitter and a Mach–Zehnder interferometer [2, 5, 6], Wheeler's delayed choice experiments [2, 7, 8], a quantum eraser experiment [2, 9], two-beam single-photon interference experiments and the single-photon interference experiment with a Fresnel biprism [2, 3, 10], quantum cryptography protocols [11], the Hanbury Brown–Twiss experiments [2, 12], universal quantum computation [13, 14], Einstein–Podolsky–Rosen–Bohm (EPRB) experiments [2, 3, 15–20], the propagation of electromagnetic plane waves through homogeneous thin films and stratified media [2, 21], and several single-neutron interferometry experiments [3, 4].

In this paper, we demonstrate that the same approach provides an event-by-event description of recent neutron experiments [22, 23] devised to test (generalizations of) Heisenberg's uncertainty principle. As the event-by-event simulation generates data consistent with the statistical predictions of quantum theory, they also satisfy the inequalities that are generalizations of Heisenberg's uncertainty principle. However, as the event-by-event simulation does not resort to concepts of quantum theory, it seems to provide support to the idea that many predictions of quantum theory may be deduced using a 'classical' statistical theory [24–36].

The experiment and the quantum theoretical description

A block diagram of the neutron experiment designed for testing uncertainty relations [22, 23] is shown in figure 1. Conceptually, this experiment exploits two different physical phenomena: the motion of a magnetic moment in a static magnetic field and the beam filtering by a spin analyzer performing a Stern–Gerlach–like selection of the neutrons based on the direction of their magnetic moments.

A magnetic moment $\mathbf{S}$ in an external, static magnetic field $B\mathbf{e}$ experiences a rotation about the direction of the unit vector $\mathbf{e}$. For a spin-1/2 particle, a unitary transformation that corresponds to such a rotation is given by

$$U_{\mathbf{b}}(\varphi) = \mathrm{e}^{\mathrm{i}\gamma t B\mathbf{S}\cdot\mathbf{e}} = \mathrm{e}^{\mathrm{i}\varphi\boldsymbol{\sigma}\cdot\mathbf{e}}, \tag{1}$$

where γ is the gyromagnetic ratio of the particle, t is the time of the particle interaction with the magnetic field, the variable $\varphi = \gamma t B/2$ is the angle of rotation, and $\boldsymbol{\sigma} = (\sigma_x, \sigma_y, \sigma_z)$ are the Pauli-spin operators.

An ideal spin analyzer passes all particles having their spin polarized 'up' in some direction, stops all particles having their spin 'down' and passes only some particles polarized differently, changing at the same time their polarization to the direction 'up'. The detailed discussion of successive spin filtering experiments may be found on pages 246–252 in [37]. An ideal spin analyzer directed along the unit vector $\mathbf{n}$ is represented by the projection operator

$$M(S, \mathbf{n}) = \frac{\mathbb{1} + S\boldsymbol{\sigma}\cdot\mathbf{n}}{2}, \tag{2}$$

where $\mathbb{1}$ is the unit matrix and $S = \pm 1$ selects one of the two possible alignments of the spin polarizer along $\mathbf{n}$ (see [22, 23]). For $S = 1$ it passes the particles with spin polarized 'up' and for $S = -1$ the particles with spin polarized 'down'.

Using equations (1) and (2), it is straightforward to construct the quantum theoretical description of each of the three stages in the experimental setup. By choosing appropriate configurations of various devices used in the neutron experiment, we may estimate various joint filtering probabilities in four experiments labeled $(S1, S2)$: $(1, 1), (-1, 1), (1, -1)$ and $(-1, 1)$.

For configurations chosen in [22, 23] the following quantum theoretical description may be given. Neutrons are prepared in an initial state represented by the density matrix

$$\rho = \frac{\mathbb{1} + \boldsymbol{\sigma}\cdot\mathbf{a}}{2}. \tag{3}$$

Taking account of all components of the setup of the neutron experiment [22, 23] and the quantum theoretical description of successive filtering experiments [37], one can show that

$$P(S_1, S_2|\mathbf{a}) = \frac{1 + \sin\phi S_1 S_2}{4} + \frac{(S_1 + S_2\sin\phi)(a_x\cos\phi + a_y\sin\phi)}{4}. \tag{4}$$

One may say that the neutron experiment performs successive measurements of the operators $\sigma_\phi = \sigma_x\cos\phi + \sigma_y\sin\phi$ and σ_y, their eigenvalues being S_1 and S_2, respectively. Note that these two operators do not commute unless $\cos\phi = 0$ and that the observed eigenvalues S_1 and S_2 of these two operators

are correlated, as is evident from the contribution $\sin\phi S_1 S_2/4$ in equation (4).

From equation (4), the expectation values of the various spin operators follow immediately. Specifically, we have

$$\begin{aligned}\left\langle\sigma_\phi\right\rangle_{\mathbf{a}} &= \sum_{S_1,S_2=\pm1} S_1 P\left(S_1, S_2|\mathbf{a}\right) = a_x\cos\phi + a_y\sin\phi,\\ \left\langle\sigma_y\right\rangle_{\mathbf{a}} &= \sum_{S_1,S_2=\pm1} S_2 P\left(S_1, S_2|\mathbf{a}\right) = \sin\phi\left\langle\sigma_\phi\right\rangle_{\mathbf{a}},\end{aligned} \tag{5}$$

and as $\sigma_\phi^2 = \sigma_y^2 = 1$, the variances $\left\langle\sigma_\phi^2\right\rangle_{\mathbf{a}} - \left\langle\sigma_\phi\right\rangle_{\mathbf{a}}^2$ and $\left\langle\sigma_y^2\right\rangle_{\mathbf{a}} - \left\langle\sigma_y\right\rangle_{\mathbf{a}}^2$ are completely determined by equation (5).

Event-by-event simulation

A minimal, discrete-event simulation model of single-neutron experiments requires a specification of the information carried by the neutrons, of the algorithm that simulates the source and the devices used in the experimental setup (see figure 1), and of the procedure for analyzing the data.

The messenger: A neutron is regarded as a messenger carrying a message. In principle, there is a lot of freedom for specifying the content of the message, the only criterion being that in the end, the simulation should reproduce the results of real laboratory experiments. We adopt Occam's razor as a guiding principle to determine which kinds of data the messenger should carry and we use the minimal amount of data.

The pictorial description that will be used in the following should not be taken literally: it is only meant to help visualize, in terms of concepts familiar from macroscopic physics, the minimal amount of data that the messenger should carry.

Picturing the neutron as a tiny magnet, we can use the spherical coordinates θ and φ to specify the direction of its magnetic moment

$$\mathbf{m} = \left(\cos\varphi\sin\theta, \sin\varphi\sin\theta, \cos\theta\right)^{\mathrm{T}}, \tag{6}$$

relative to the fixed frame of reference defined by the static magnetic field $B_0\mathbf{z}$. The messenger should also be aware of the time that it takes to move from one point in space to another. The time of flight and the direction of the magnetic moment are conveniently encoded in a message of the type [3, 4]

$$\mathbf{u} = \left(\mathrm{e}^{\mathrm{i}\psi^{(1)}}\cos\left(\theta/2\right), \mathrm{e}^{\mathrm{i}\psi^{(2)}}\sin\left(\theta/2\right)\right)^{\mathrm{T}}, \tag{7}$$

where $\psi^{(i)} = \omega t + \delta_i$, for $i = 1, 2$, and $\varphi = \delta_1 - \delta_2 = \psi^{(1)} - \psi^{(2)}$. Within the present model, the state of the neutron, that is the message, is completely described by the angles $\psi^{(1)}$, $\psi^{(2)}$ and θ and by rules (to be specified) by which these angles change as the neutron travels through the network of devices. This model suffices for reproducing the results of single-neutron interference and entanglement experiments and of their idealized quantum theoretical descriptions [3, 4].

In specifying the message of equation (7), we exploited the isomorphism between the algebra of Pauli matrices and rotations in three-dimensional space, not because the former connects to quantum mechanics but just because we find this representation most convenient for our simulation work [2–4]. The direction of the magnetic moment follows from equation (7) through

$$\mathbf{m} = \mathbf{u}^T\boldsymbol{\sigma}\mathbf{u}. \tag{8}$$

A messenger with message $\mathbf{u}$ at time t and position $\mathbf{r}$ that travels with velocity v, along the direction $\mathbf{q}$ during a time interval $t' - t$, changes its message according to $\psi^{(i)} \leftarrow \psi^{(i)} + \omega\left(t' - t\right)$ for $i = 1, 2$, where ω is an angular frequency which is characteristic for a neutron that moves with a fixed velocity v. In a monochromatic beam of neutrons, all neutrons have the same value of ω [38].

In the presence of a magnetic field $\mathbf{B} = \left(B_x, B_y, B_z\right)$, the magnetic moment rotates about the direction of $\mathbf{B}$ according to the classical equation of motion

$$\frac{\mathrm{d}\mathbf{m}}{\mathrm{d}t} = \mathbf{m}\times\mathbf{B}. \tag{9}$$

Hence, as the messenger passes a region in which a magnetic field is present, the message $\mathbf{u}$ changes into the message

$$\mathbf{u} \leftarrow \mathrm{e}^{\mathrm{i}g\mu_N T\boldsymbol{\sigma}\cdot\mathbf{B}/2}\mathbf{u}, \tag{10}$$

where g denotes the neutron g-factor, μ_N the nuclear magneton, and T the time during which the messenger experiences the magnetic field.

In the event-based simulation of the experiment shown in figure 1, the time of flight T determines the angle of rotation of the magnetic moment through equation (10) and can, so to speak, be eliminated by expressing all operations in terms of rotation angles. However, this simplification is no longer possible in the event-based simulation of single-neutron interference and entanglement experiments [3, 4].

The source: When the source creates a messenger, its message needs to be initialized. This means that three angles $\psi^{(1)}$, $\psi^{(2)}$ and θ need to be specified. In practice, instead of implementing stage 1 it is more efficient to prepare the messengers such that the corresponding magnetic moments are along a specified fixed direction. For instance, to mimic fully coherent, spin-polarized neutrons that enter stage 2 with their spin along the x-axis, the source would create messengers with $\theta = \pi/2$, and without loss of generality, $\psi^{(1)} = \psi^{(2)} = 0$.

The spin flipper: The spin flipper rotates the magnetic moment by an angle $\pi/2$ about the x-axis.

The spin analyzer: The simulation model of this component is very simple: it lets the messenger pass if

$$r \leqslant \frac{1 + m_z S}{2}, \tag{11}$$

where $0 < r < 1$ is a uniform pseudo-random number and, as before, $S = \pm1$ labels the orientation of the spin analyzer. If equation (11) is not satisfied, the messenger is destroyed.

The detector: As a messenger enters the detector, the detection count is increased by 1 and the messenger is destroyed. The detector counts all incoming messengers. Hence, we assume that the detector has a detection efficiency of 100%. This is a good model of real neutron detectors, which can have a detection efficiency of 99% or more [39].

The simulation procedure and data analysis: First, we establish the correspondence between the initial message $\mathbf{u}_{\text{initial}}$ and the description in terms of the density matrix equation (3). For instance we remove all devices from stages 1 and 2 and simply count the number of messages that pass SA3 with $S_2 = 1$. It follows from equation (11) that the relative frequency of counts is given by m_z, the projection of the message onto the z-axis. In other words, we would infer from the data that in a quantum theoretical description, the z-component of the density matrix a_z is equal to m_z. By performing rotations of the original message, it follows by the same argument that $\mathbf{a} = \mathbf{m}_{\text{initial}}$.

For each pair of settings (S_1, S_2) of the spin analyzers (SA2, SA3) and each position of the pair of spin flippers (SF2, SF3) represented by a rotation of ϕ about the z-axis, the source sends N messengers through the network of devices shown in figure 1. The source only creates a new messenger if (i) the previous messenger has been processed by the detector or (ii) the messenger was destroyed by one of the spin analyzers. In other words, direct communication between messengers is excluded. As a device in the network receives a messenger, it processes the message according to the rules specified earlier and sends the messengers with the new message to the next device in the network. If the device is a spin analyzer, it may happen that the messenger is destroyed. The detector counts all messengers that pass SA3 and destroys these messengers.

For a sequence of N messengers all carrying the same initial message $\mathbf{a} = \mathbf{m}_{\text{initial}}$, this procedure yields a count $N(S_1, S_2|\mathbf{a})$ (recall that ϕ is fixed during each sequence of N events). Repeating the procedure for the four pairs of settings yields the relative frequencies

$$F(S_1, S_2|\mathbf{a}) = \frac{N(S_1, S_2|\mathbf{a})}{\sum_{S_1,S_2=\pm 1} N(S_1, S_2|\mathbf{a})}. \tag{12}$$

Note that the numerator in equation (12) is not necessarily equal to N because messengers may be destroyed when they enter a spin analyzer. From equation (12) we compute

$$\langle S_1 \rangle = \sum_{S_1,S_2=\pm 1} S_1 F(S_1, S_2|\mathbf{a}), \tag{13}$$

$$\langle S_2 \rangle = \sum_{S_1,S_2=\pm 1} S_2 F(S_1, S_2|\mathbf{a}), \tag{14}$$

$$\langle S_1 S_2 \rangle = \sum_{S_1,S_2=\pm 1} S_1 S_2 F(S_1, S_2|\mathbf{a}). \tag{15}$$

Validation: The event-based model reproduces the results of the quantum theoretical description if, within the usual statistical fluctuations, we find that $F(S_1, S_2|\mathbf{a}) \approx P(S_1, S_2|\mathbf{a})$ with $P(S_1, S_2|\mathbf{a})$ given by equation (4). This correspondence is most easily established by noting that for fixed ϕ and $\mathbf{a}$, the three expectations of equations (13)–(15) completely determine equation (12) and that, likewise, the quantum theoretical distribution of equation (4) is completely determined by the expectations of equations (13)–(15) with $F(S_1, S_2|\mathbf{a})$ replaced by $P(S_1, S_2|\mathbf{a})$. In other words, for the event-based model to reproduce the results of the quantum theoretical description of the neutron experiment [22, 23], it is necessary and sufficient that the simulation results for equations (13)–(15) are in agreement with the quantum theoretical results (see equation (5)) $\langle S_1 \rangle = a_x \cos\phi + a_y \sin\phi$, $\langle S_2 \rangle = \sin\phi \langle S_1 \rangle$, and $\langle S_1 S_2 \rangle = \sin\phi$. As figure 2 shows, the results of

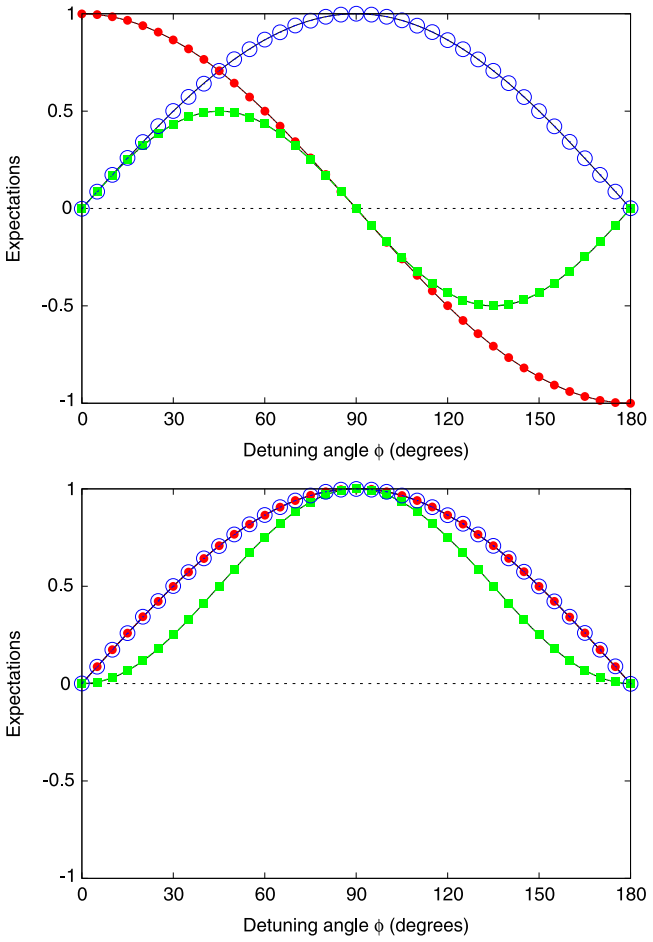

Figure 2. Results for the expectations $\langle S_1 \rangle$ (red solid circles), $\langle S_2 \rangle$ (green solid squares), and $\langle S_1 S_2 \rangle$ (blue open circles) as obtained by the event-by-event simulation of the neutron experiment [22, 23]. The solid lines represent the corresponding quantum theoretical prediction. Top: incoming particles have magnetization $\mathbf{a} = (1, 0, 0)$. Bottom: incoming particles have magnetization $\mathbf{a} = (0, 1, 0)$. For each pair of settings (S_1, S_2) of the spin analyzers (SA2, SA3) and each position of the pair of spin flippers (SF2, SF3) represented by a rotation of ϕ about the z-axis, referred to as the detuning angle in [22, 23], the simulation consists of sending $N = 1000\,000$ messengers ('neutrons') into stage 2.

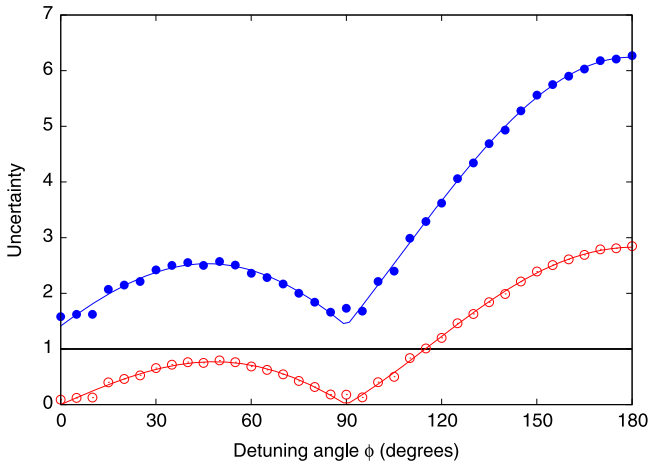

Figure 3. Simulation results for the uncertainties $\varepsilon(A)\eta(B) + \varepsilon(A)\sigma(B) + \sigma(A)\eta(B)$ (blue solid circles) and $\varepsilon(A)\eta(B)$ (red open circles) as obtained from the event-by-event simulations of the single-neutron experiment [22, 23]. The lines through the data points represent the corresponding quantum theoretical prediction. The solid horizontal line represents the lower bound in equation (16). It is clear that the naive application of the Heisenberg uncertainty relation, $\varepsilon(A)\eta(B) \geqslant 1$, is at odds with the prediction of quantum theory and the event-based simulation, and with the experimental data (not shown, but see [22, 23]). On the other hand, the results of the event-based simulation and the experimental data (not shown, but see [22, 23]) comply with the inequality equation (16). For each initial state, each pair of settings (S_1, S_2) of the spin analyzers (SA2, SA3) and each position of the pair of spin flippers (SF2, SF3) represented by a rotation of ϕ about the z-axis, referred to as the detuning angle in [22, 23], the simulation consists of sending $N = 10\,000$ messengers ('neutrons') into stage 2.

event-based simulations are in excellent agreement with the predictions of the quantum theoretical description of equation (4) of the neutron experiment [22, 23]. Using the root mean square error as a measure for the difference between the simulation data and the quantum theoretical prediction, we find that for each of the expectations shown in figure 2 the root mean square error is less than 0.01 and 0.001 for $N = 10\,000$ and $N = 1000\,000$ events, respectively.

Summarizing: the event-based simulation model of the neutron experiment [22, 23] presented in this section does not rely, in any sense, on concepts of quantum theory, yet it reproduces all features of the quantum theoretical description of the experiment. Although the event-based model is classical in nature, it is not classical in the sense that it can be described by classical Hamiltonian dynamics, the reason being that the operation of the spin analyzers requires a probabilistic description.

Uncertainty relations

The purpose of the neutron experiment [22, 23] was to test an error–disturbance uncertainty relation proposed by Ozawa [40]. By introducing particular definitions of the measurement error $\varepsilon(A)$ of an operator A and the disturbance $\eta(B)$ of an operator B, Ozawa showed that

$$\varepsilon(A)\eta(B) + \varepsilon(A)\Delta(B) + \Delta(A)\eta(B) \geqslant \frac{1}{2}\left|\left\langle [A, B]\right\rangle\right|, \quad (16)$$

where

$$\varepsilon^2(A) = \left\langle (M_A - A)^2\right\rangle, \quad (17)$$

$$\eta^2(B) = \left\langle (M_B - B)^2\right\rangle, \quad (18)$$

$$\Delta^2(A) = \left\langle A^2\right\rangle - \left\langle A\right\rangle^2, \quad (19)$$

$$\Delta^2(B) = \left\langle B^2\right\rangle - \left\langle B\right\rangle^2, \quad (20)$$

and M_A and M_B represent the operators of different measuring devices (implying that $[M_A, M_B] = 0$) that allow us to read off the value of the measurement for A and B, respectively. Thereby it is assumed that $\langle M_A\rangle = \langle A\rangle$ and $\langle M_B\rangle = \langle B\rangle$, that is that the measurements of A and B are unbiased, implying that $\varepsilon(A) = \Delta(M_A - A)$ and $\eta(B) = \Delta(M_B - B)$.

If the state of the spin-1/2 system is described by the density matrix $\rho = |\mathbf{z}\rangle\langle\mathbf{z}|$, for appropriate choice of the operators A, M_A, B and M_B one obtains

$$\varepsilon^2(A) = 2 - 2\sum_{S_1,S_2=\pm1} S_1 P\left(S_1, S_2|\mathbf{a} = (1, 0, 0)\right)$$
$$\eta^2(B) = 2 - 2\sum_{S_1,S_2=\pm1} S_2 P\left(S_1, S_2|\mathbf{a} = (0, 1, 0)\right), \quad (21)$$

where $P(S_1, S_2|\mathbf{a})$ is given by equation (4).

In the neutron experiment [22, 23] and therefore also in our event-based simulation, the numerical values of $\varepsilon(A)$ and $\eta(B)$ are obtained by counting detection events. We have

$$\varepsilon^2(A) \approx 2 - 2\frac{\sum_{S_1,S_2=\pm1} S_1 N(S_1, S_2|\mathbf{x})}{\sum_{S_1,S_2=\pm1} N(S_1, S_2|\mathbf{x})}$$
$$\eta^2(B) \approx 2 - 2\frac{\sum_{S_1,S_2=\pm1} S_2 N(S_1, S_2|\mathbf{y})}{\sum_{S_1,S_2=\pm1} N(S_1, S_2|\mathbf{y})}, \quad (22)$$

where $N(S_1, S_2|\mathbf{a})$ denotes the count for the case in which the direction of the magnetic moment of the incoming neutrons (after stage 1) is $\mathbf{a}$ and the analyzers SA2 and SA3 are along the directions S_1 and S_2, respectively.

As shown in [22, 23], the neutron counts observed in the single-neutron experiment yield numerical values of $\varepsilon(A)\eta(B) + \varepsilon(A)\sigma(B) + \sigma(A)\eta(B)$ which are in excellent agreement with the quantum theoretical prediction.

We already checked that the 'classical' event-based simulation model produces results which, within the statistical errors, agree with the probabilities predicted by quantum theory. Therefore it is to be expected that the data generated

by the event-by-event simulation also satisfy the universally valid error–disturbance uncertainty relation equation (16). As shown in figure 3, this is indeed the case and, also as expected, the data produced by the event-based simulation also violate the naively interpreted Heisenberg uncertainty relation

$$\varepsilon(A)\eta(B) \geqslant \frac{1}{2}\left|\left\langle [A, B]\right\rangle\right|. \tag{23}$$

Finally, for the sake of completeness, we show that the event-by-event simulation produces data which comply with the standard Heisenberg–Robertson uncertainty relation $\Delta(\sigma_x)\Delta(\sigma_y) \geqslant \left|\left\langle \sigma_z\right\rangle\right|$ which also should be universally valid. Without loss of generality, the state of the spin-1/2 particle may be represented by the density matrix equation (3) also if it is interacting with other degrees of freedom. More explicitly, the inequality $\Delta(\sigma_x)\Delta(\sigma_y) \geqslant \left|\left\langle \sigma_z\right\rangle\right|$ reads

$$\left(1-\left\langle \sigma_x\right\rangle^2\right)\left(1-\left\langle \sigma_y\right\rangle^2\right) \geqslant \left\langle \sigma_z\right\rangle^2, \tag{24}$$

or, using equation (3),

$$\left(1-a_x^2\right)\left(1-a_y^2\right) \geqslant a_z^2. \tag{25}$$

The last inequality also trivially follows from the constraint $a_x^2 + a_y^2 + a_z^2 \leqslant 1$.

The simulation procedure that we use is as follows.

1. Loop over the values $(\mathbf{m}_{\text{initial}})_z = a_z = -1, \ldots, 1$ in small steps, e.g. in steps of 0.05.
2. Generate a uniform pseudo-random number $0 < r < 1$. Compute $(\mathbf{m}_{\text{initial}})_x = a_x = \sqrt{1-a_z^2}\cos(2\pi r)$ and $(\mathbf{m}_{\text{initial}})_y = a_y = \sqrt{1-a_z^2}\sin(2\pi r)$. This step yields a direction of the magnetization $\mathbf{m}_{\text{initial}}$ which is chosen randomly in the x–y plane.
3. Generate N messengers with message $\mathbf{m}_{\text{initial}}$ and send them through a spin analyzer aligned along the x-direction. Count the messengers that pass the spin analyzer. Repeat this procedure for spin analyzers aligned along the $-x$-, $\pm y$- and $\pm z$-directions. Processing the N messengers yields the counts $N(\mathbf{x}|\mathbf{a})$, $N(-\mathbf{x}|\mathbf{a})$, etc.
4. Compute the averages $\langle\sigma_x\rangle \approx \left(N(\mathbf{x}|\mathbf{a}) - N(-\mathbf{x}|\mathbf{a})\right)/\left(N(\mathbf{x}|\mathbf{a}) + N(-\mathbf{x}|\mathbf{a})\right)$, etc.
5. Go to the next step as long as $a_z \leqslant 1$.
6. Plot the results for $\left(1-\left\langle \sigma_x\right\rangle^2\right)\left(1-\left\langle \sigma_y\right\rangle^2\right)$ and $\left\langle \sigma_z\right\rangle^2$ as a function of a_z.

The results of the event-based simulation are shown in figure 4. Within the usual statistical errors, the classical, statistical model produces data which comply with the Heisenberg–Robertson uncertainty relation, equation (25).

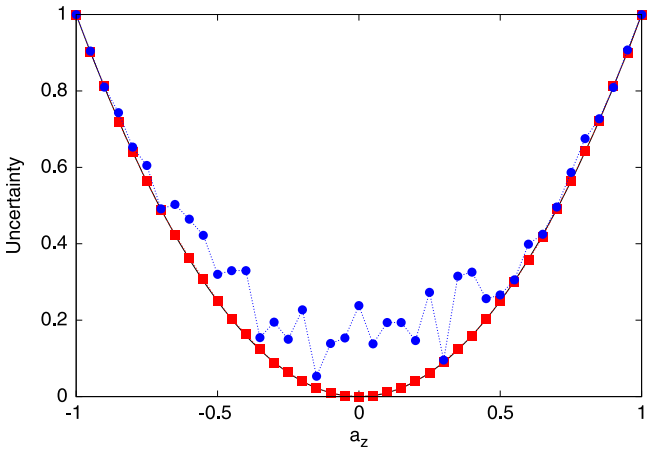

Figure 4. Event-based simulation results for $(1-\left\langle \sigma_x\right\rangle^2)(1-\left\langle \sigma_y\right\rangle^2)$ (blue circles) and $\left\langle \sigma_z\right\rangle^2$ (red squares) for different values of $-1 \leqslant a_z \leqslant 1$. The solid black line represents the quantum theoretical lower bound a_z^2. For each value of a_z, the initial direction of the magnetic moments is (a_x, a_y, a_z), where (a_x, a_y) is a point on the circle with radius $\sqrt{1-a_z^2}$ chosen using a uniform pseudo-random number. The fluctuations of the data $(1-\left\langle \sigma_x\right\rangle^2)(1-\left\langle \sigma_y\right\rangle^2)$ reflect the fact that the initial states with different values of a_z are uncorrelated. For each value of a_z, $N = 100\,000$ messengers were created. The dotted line is a guide to the eyes only.

Discussion

We have shown that a genuine classical event-based model can produce events such that their statistics satisfies the (generalized) Heisenberg–Robertson uncertainty relation which is often associated with truly quantum mechanical behavior.

The argument that in the non-quantum, event-based model, the direction of the magnetic moment is known exactly and therefore cannot be subject to uncertainty is incorrect in that it ignores the fact that the model of the spin analyzers introduces (through the use of pseudo-random numbers) uncertainty in the outcomes.

In fact, as is well-known, the variance of any statistical experiment (including those that are interpreted in terms of quantum theory) satisfies the Cramér–Rao bound, a lower bound on the variance of estimators of a parameter of the probability distribution in terms of the Fisher information [41]. The Cramér–Rao bound contains, as a special case, Robertson's inequality $\Delta(x)\Delta(p) \geqslant \hbar/2$ [24, 27, 31–33, 42]. The observation that a classical statistical model produces data that comply with 'quantum theoretical' uncertainty relations is a manifestation of this general mathematical result. From the viewpoint of real data sets, the uncertainty relations provide theoretical bounds on the statistical uncertainties in the data and, as shown by our event-based simulation of the neutron experiment [22, 23], are not necessarily a signature of quantum fluctuations, wave–particle duality, etc. Uncertainty relations seem to express only a

general property of probability distributions describing the results of incompatible experimental setups used to measure two incompatible random variables in any domain of science.

Acknowledgments

We would like to thank Koen De Raedt, Karl Hess, and Seiji Miyashita for many stimulating discussions and two anonymous referees for their suggestions for improving the presentation of our work.

References

[1] Bohr N 1999 (*Complementarity Beyond Physics (1928–1962) Niels Bohr Collected Works*) ed D Favrholdt vol 10 (Amsterdam: Elsevier) pp 155–60
[2] Michielsen K, Jin F and De Raedt H 2011 *J. Comput. Theor. Nanosci.* **8** 1052
[3] De Raedt H and Michielsen K 2012 *Ann. Phys. (Berlin)* **524** 393
[4] De Raedt H, Jin F and Michielsen K 2012 *Quantum Matter* **1** 1
[5] De Raedt H, De Raedt K and Michielsen K 2005 *Europhys. Lett.* **69** 861
[6] De Raedt K, De Raedt H and Michielsen K 2005 *Comput. Phys. Comm.* **171** 19
[7] Zhao S, Yuan S, De Raedt H and Michielsen K 2008 *Europhys. Lett.* **82** 40004
[8] Michielsen K, Yuan S, Zhao S, Jin F and De Raedt H 2010 *Physica* E **42** 348
[9] Jin F, Zhao S, Yuan S, De Raedt H and Michielsen K 2010 *J. Comput. Theor. Nanosci.* **7** 1771
[10] Jin F, Yuan S, De Raedt H, Michielsen K and Miyashita S 2010 *J. Phys. Soc. Jpn.* **79** 074401
[11] Zhao S and De Raedt H 2008 *J. Comput. Theor. Nanosci.* **5** 490
[12] Jin F, De Raedt H and Michielsen K 2010 *Commun. Comput. Phys.* **7** 813
[13] De Raedt H, De Raedt K and Michielsen K 2005 *J. Phys. Soc. Jpn. Suppl.* **76** 16
[14] Michielsen K, De Raedt K and De Raedt H 2005 *J. Comput. Theor. Nanosci.* **2** 227
[15] De Raedt K, Keimpema K, De Raedt H, Michielsen K and Miyashita S 2006 *Eur. Phys. J.* B **53** 139
[16] De Raedt H, De Raedt K, Michielsen K, Keimpema K and Miyashita S 2007 *J. Phys. Soc. Jpn.* **76** 104005
[17] De Raedt K, De Raedt H and Michielsen K 2007 *Comp. Phys. Comm.* **176** 642
[18] De Raedt H, De Raedt K, Michielsen K, Keimpema K and Miyashita S 2007 *J. Comput. Theor. Nanosci.* **4** 957
[19] De Raedt H, Michielsen K, Miyashita S and Keimpema K 2007 *Eur. Phys. J.* B **58** 55
[20] Zhao S, De Raedt H and Michielsen K 2008 *Found. Phys.* **38** 322
[21] Trieu B, Michielsen K and De Raedt H 2011 *Comput. Phys. Comm.* **182** 726
[22] Erhart J, Sponar S, Sulyok G, Badurek G, Ozawa M and Hasegawa Y 2012 *Nat. Phys.* **8** 185
[23] Sulyok G, Sponar S, Erhart J, Badurek G, Ozawa M and Hasegawa Y 2013 *Phys. Rev.* A **88** 022110
[24] Frieden B R 1989 *Am. J. Phys.* **57** 1004
[25] Reginatto M 1998 *Phys. Rev.* A **58** 1775
[26] Hall M J W 2000 *Phys. Rev.* A **62** 012107
[27] Frieden B R 2004 *Science from Fisher Information: A Unification* (Cambridge: Cambridge University Press)
[28] Khrennikov A Y 2009 *Contextual Approach to Quantum Formalism* (Berlin: Springer)
[29] Khrennikov A Y 2011 *J. Comp. Theor. Nanosci.* **8** 1006
[30] Khrennikov A Y, Nilsson B and Nordebo S 2011 *J. Phys. Conf. Ser.* **361** 012030
[31] Kapsa V, Skála L and Chen J 2010 *Physica* E **42** 293
[32] Skála L, Čížêk J and Kapsar V 2011 *Ann. Phys.* **326** 1174
[33] Kapsa V and Skála L 2011 *J. Comput. Theor. Nanosci.* **8** 998
[34] Klein U 2012 *Am. J. Phys.* **80** 1009
[35] Klein U and 2010 *Phys. Res. Int.* **2010** 808424
[36] Flego S P, Plastino A and Plastino A R 2012 *Int. Res. J. Pure & Appl. Chem.* **2** 25
[37] Ballentine L E 2003 *Quantum Mechanics: A Modern Development* (Singapore: World Scientific)
[38] Rauch H and Werner S A 2000 *Neutron Interferometry: Lessons in Experimental Quantum Mechanics* (London: Clarendon)
[39] Kroupa G, Bruckner G, Bolik O, Zawisky M, Hainbuchner M, Badurek G, Buchelt R J, Schricker A and Rauch H 2000 *Nucl. Instrum. Methods Phys. Res.* A **440** 604
[40] Ozawa M 2003 *Phys. Rev.* A **67** 042105
[41] van Trees H L 1968 *Detection, Estimation, and Modulation Theory (Part I)* (New York: John Wiley)
[42] Stam A J 1959 *Inf. Control* **2** 101